Identification of phytochemical inhibitors against main protease of COVID-19 using molecular modeling approaches

Anuj Kumar (anujbioinfo91@gmail.com)
Uttarakhand Council for Biotechnology, Dehradun, India https://orcid.org/0000-0002-5023-7618
Gourav Choudhir
CCS University, Meerut, UP-250004, India
Sanjeev Kumar Shukla
Government Medical College, Haldwani, Nanital, Uttarakhand-263139, India
Mansi Sharma
Academy of Biological Science & Research Foundation (ABSRF), Udaipur, Rajasthan-313001, India
Pankaj Tyagi
Noida Institute of Engineering & Technology Greater Noida, UP-201306, India
Arvind Bhushan
IIHMR University, Jaipur, Rajsthan-302029, India
Madhu Rathore
Academy of Biological Science & Research Foundation (ABSRF), Udaipur, Rajasthan-313001, India

Research Article

Keywords: COVID-19, protease, ursolic acid, carvacrol, oleanolic acid

Posted Date: May 26th, 2020

DOI: https://doi.org/10.21203/rs.3.rs-31210/v1

Version of Record: A version of this preprint was published on January 25th, 2021. See the published version at https://doi.org/10.1186/s12302-020-00452-0.

Abstract

Severe acute respiratory syndrome coronavirus-2 (SARS-CoV-2) is a novel corona virus that causes corona virus disease 2019 (COVID-19). The COVID-19 rapidly spread across the nations with high mortality rate even as very little is known to contain the virus at present. In the current study, we report novel natural metabolites namely, ursolic acid, carvacrol and oleanolic acid as the potential inhibitors against main protease (M^{pro}) of COVID-19 by using integrated molecular modeling approaches. From a combination of molecular docking and molecular dynamic (MD) simulations, we found three ligands bound to protease during 50 ns of MD simulations. Furthermore, the molecular mechanic/generalized/Born/Poisson-Boltzmann surface area (MM/G/P/BSA) free energy calculations showed that these chemical molecules have stable and favourable energies causing strong binding with binding site of M^{pro} protein. All these three molecules, namely, ursolic acid, carvacrol and oleanolic acid, have passed the ADME (Absorption, Distribution, Metabolism, and Excretion) property as well as Lipinski's rule of five. The study provides a basic foundation and suggests that the three phytochemicals, *viz.* ursolic acid, carvacrol and oleanolic acid could serve as potential inhibitors in regulating the M^{pro} protein's function and controlling viral replication.

1. Introduction

Coronavirus disease (COVID-19) is a respiratory infectious disease caused by a novel virus strain, SARS-CoV-2 (Su et al., 2016; Salata et al., 2019; Hemida & Ba Abduallah, 2020; Seah & Agarwal, 2020; Boopathi et al., 2020; Sarma et al., 2020). In the past two decades, two other coronavriruses have caused global outbreaks, namely SARS-CoV (2002-2003) and Middle East respiratory syndrome coronavirus (2012-present) (de Wit et al., 2016; Wu et al., 2020; Wang et al., 2020; Yuan et al. 2020; Gupta et al., 2020). The Coronavirus Study Group (CSG) taxonomists working under the aegis of International Committee on Taxonomy of Viruses (ICTV) coined the nomenclature of SARS-COV-2 based on its 82% identity to the SARS coronavirus (SARS-CoV) genome (Coronaviridae Study Group of the International Committee on Taxonomy of Viruses, 2020; Hasan et al., 2020). Whole genome functional analysis revealed that both viruses phylogenetically belong to clade b of the genus *Betacoronavirus* (WHO, 2020; Chan et al., 2020; Murlidharan et al., 2020). The very first case of the novel COVID-19 was originally reported in Wuhan, Hubei Province, China, and has quickly spread over the 212 countries of the world (Xu *et al.,* 2020; Mackenzie & Smith, 2020; Enayatkhani et al., 2020; Elmezayen et al., 2020). This contagious disease has led to over 4, 098, 018 confirmed cases and 283,271fatalities as on May 12, 2020; https://covid19.who.int/). The number of cases across the globe is increasing abruptly, and so far, there is no standard drug has proved to be effective for COVID-19 disease that have high mortality rate in immunocompromised patients (Weiss & Murdoch, 2020; Bhatraju et al., 2020; Aanouz et a., 2020). On 30 January, this respiratory infectious disease has been declared as a Public Health Emergency of International Concern by the World Health Organization (WHO) (Mackenzie & Smith, 2020; https://www.who.int/).

The SARS-CoV-2 genome is about 30kb in size (29, 903 nucleotides) and encodes as many as 14 open reading frames (ORFs) (Gorden et al., 2020; Woo et al., 2020; Chen et al., 2020; Elfiky and Azzam, 2020). At the 5' end of the viral genome, Orf1a/Orf1ab encodes several proteins, which are auto-proteolytically processed into 16 non-structural proteins (Nsp1-16) and form the replicase/ transcriptase complex (RTC). Whereas, 3' endencode structural viral proteins; spike (S), membrane (M), envelope (E) and nucleocapsid (N), and nine putative accessory factors. On the other hand, protease enzyme called the M^{pro} or also $3CL^{pro}$, play a crucial role in the life cycle of COVID-19 replication and maturation (Wu et al., 2020; Khan et al., 2020; Pant et al., 2020; Joshi et al., 2020). It has been demonstrated that no part of COVID-19 is more exposed than its main protease, as belongs to non-structural class proteins of the viral genome (Zhang et al., 2020; Enmmozi et al., 2020). Zhang et al., 2020 determined the three-dimensional crystal structure, at 1.75 Å resolution, of the M^{pro} of SARS-CoV-2 using x-ray crystallography.

Like other coronaviruses, the 3D structure of $3CL^{pro}$ of SARS-COV-2 possesses three functional domains (Jin et al., 2020; Khan et al., 2020). The length of domain I, II, and III ranges from 8-101, 102-184, 201-306 amino acid residues, respectively. Among them, domain I and II are essentially beta-barrels and similar to the chymotrypsin. While, structural composition of domain III mainly consists of alpha-helices (Anand et al., 2005; Yang et al., 2005; Lu et al., 2006; Jin et al., 2020), protease has been characterized as one of the potential drug targets among coronaviruses (Anand et al., 2003). In this sense, many recent studies suggested that the selection of various FDA-approved antiviral compounds may yield promising results against COVID-19 infection (Chang et al., 2016; Chang et al., 2020; Contini, 2020; Gonzalez-Paz et al., 2020; Khan et al., 2020; Elfiky, 2020a;b; Islam et al., 2020; Sinha et al., 2020; Wahedi et al., 2020; Kundu et al., 2020; Das et al., 2020; Abdelli et al., 2020). Chang et al., 2020 reported that chloroquine, an older antimalarial drug, has ability to inhibit the viral 3CL-protease activity. As crystal structure of protease provides a foundation for design of improved α-ketoamide inhibitors (Zhang et al., 2020), the capability of chloroquine to inhibit the protease activity its uses has been recommended in different countries including China, USA and India for the treatment of COVID-19 (Devaux et al., 2020; Gonzalez-Paz et al., 2020; Wang et al., 2020). However, many studies questioned the safety and reported the severe adverse effects of chloroquine (Wang et al., 2020; Kaisari & Borruat, 2020).

Ancient Indian scriptures including Rig-Veda, Atherveda, and Charka Sanhita demonstrated abundant benefits of plants for the treatment of various human aliments (Kumar et al., 2018). Plants are a remarkable natural source of high value alkaloids, flavonoids, phenols, chalcones, coumarines, lignans, polyketides, alkanes, alkenes, alkynes, simple aromatics, peptides, terpenes, and steroids. In the current era of drug discovery, enormous medicinal properties of plants allows the researchers to exclusively use them for the discovery of drug-like natural molecules (Panchangam et al., 2016; Jee et al., 2018; Kumar et al., 2018).

Ursolic acid (3-β-3-hydroxy-urs-12-ene-28-oic-acid) and oleanolic acid (3β-hydroxyolean-12-en-28-oic acid) are pentacyclic triterpenoid compounds with a widespread occurrence throughout the plant kingdom (Pollier & Goossens, 2012; Woźniak et al., 2015). Both molecules enrich various therapeutic properties such as antibacterial, antiviral, anticancer, antioxidant and tantimycotic activity (Jesus et al., 2015). Previous *in vitro* studies reported that these molecules exhibit antiviral activity against rotavirus, HIV, the influenza virus, hepatitis B and C viruses (Tohmé et al., 2019; Jesus et al., 2015; Khwaza et al., 2018).

Carvacrol (2-Methyl-5-(propan-2-yl)phenol) is a monoterpenoid phenol, possesses a wide range of strong antimicrobial and antiviral activity (Gilling et al., 2014; Kamalabadi et al., 2018; Marinelli et al., 2019). It is a major constituent of essential oil of plants of Labiatate family including oregano and thyme, and has been emerged as active molecule for therapeutic purpose (Hyldgaard et al., 2012). Using *in-vitro* methods, antiviral effects of carvacrol has been tested and validated on herpes simplex virus type 1, retrovirus and human respiratory syncytial virus (Kamalabadi et al., 2018).

Besides the uses of various FDA-approved antiviral compounds as mentioned above, there are many *in-silico* studies have been performed to screen the novel phytochemical molecules as a potential inhibitors of main protease of SARS-CoV-2 or develop new drugs against COVID-19 (Khan et al., 2020; Khaerunnisa et al., 2020; Qamar et al., 2020; Gonzalez-Paz et al., 2020; Sharma & Kaur, 2020; Chandel et al., 2020; Adem et al., 2020; Gentile et al., 2020; Sun et al., 2020). But there is not a single report available for the function of phytochemicals namely, ursolic acid, carvacrol and oleanolic acid derived from the antiviral herbs for the treatment of COVID-19. With the advent of molecular modeling approaches, targeted drug design may be possible and functional proteins of SARS-CoV-2 could be targeted with natural compounds to develop an effective treatment for COVID-19.

In the present study, we have targeted the protease of SARS-CoV-2 virus using available molecular modelling based methods and studied the interactions with selected natural compounds (ursolic acid, carvacrol and oleanolic acid) by molecular docking and molecular dynamics simulations followed by molecular mechanic/generalized Born/Poisson-Boltzmann surface area (MM/G/P/BSA) validation.

2. Material And Methods

A flow chart of pipeline used in present study is summarized in **Figure 1**.

2.1 Preparation of Protease

The crystal structure of COVID-19 virus main protease (M^{pro}) in complex with Z45617795 (PDB ID: 5R7Y) was solved by PanDDA analysis group (https://www.rcsb.org/structure/5R7Y). This solved protein structure (PDB ID: 5R7Y) was extracted from the RCSB-Protein Data Bank (Berman et al., 2000; Burley et al., 2019). Crystal structure of M^{pro} have dimer in form with fragment of N-(2-phenylethyl) methanesulfonamide (Z45617795) compound provides a model for identifying potent inhibitors to target COVID-19 virus M^{pro} through *in-silico* study. The protein structure was prepared by removing water atoms, hetero atoms and adding polar hydrogen atom and kollman charges on it.

2.2 Ligand Selection

Chemical structure of carvacrol (CID_10364), oleanolic acid (CID_10494) and ursolic acid (CID_64945) were extracted from PubChem database (Kim et al. 2019).

2.3 Molecular Docking

In order to find out the potential drug targets, ligand based molecular docking between phytochemical compounds *i.e.* (carvacrol, oleanolic acid and ursolic acid) and M^{pro} protein were performed using AutoDock v4.2 (Morris et al., 2009). For docking experiments, the amino acid residues including Thr24, Thr26, Asn119, Phe140, Gly143, Cys145, His163, His164, Glu166, Gln189, and Thr190 were used as the active sites. Default mode parameters were selected in AutoDock during docking analysis.

2.4 Drug Likeness

Absorption, distribution, metabolism, and excertion (ADME) calculations are important aspects of drug designing. All three ligand molecules were analysed based on the Lipinski's rule of five using (Lipinski et al., 2001), Veber's rule (Veber et al., 2002), Egan's rule (Veber et al., 2000) and polar surface area (TPSA), and number of rotatable bonds (Daina et al., 2017), were calculated using SWISSADME tool (Daina et al., 2017).

2.5 Molecular Dynamics (MD) Simulations

The structural and dynamics transition at atomistic level in the M^{pro} of COVID-19 upon binding of small molecules were investigated by using MD simulations. MD simulations were performed using GROMOS96 43a1 force field embedded in GROMACS 5.1.1 suite on LINUX based platform (Berendsen et al., 1995). For the MD simulation, we followed the protocol described by Gajula, 2008; Gajula et al., 2016; Kumar et al., 2018. PRODRG server (Schüttelkopf & van Aalten, 2004) was used to generate the topology files of small molecules. The protein complexes were solvated in the dodecahedron box with simple point charge (SPC) waters, and 4 Na^+ were added for the overall electrostatic neutrality of the system. Energy minimization of the system was performed by using the steepest descent algorithm for 50,000 iteration steps and cut-off up to 1000 kJmol−1to reduce the steric clashes. The minimization of the system was performed at two phases for 50,000 steps, where the first phase equilibrated in two different phases for 50,000 steps. The first phase of equilibration was performed with a constant number of particles, volume, and temperature (NVT), each step 2 fs, the fallowed second phase of equilibration was performed with a constant number of particles, pressure, and temperature (NPT), the ensemble at 300K. LINCS algorithm was utilized for covalent bond constraints in the equilibration steps. For the calculation of Lennard-Jones and Coulomb interactions, a 1.4 nm radius cut-off was used. Long-range electrostatics was calculated by using the Particle Mesh Ewald (PME) method with a Fourier grid spacing of 1.6Å. The temperature inside the box was regulated by using V-rescale, a modified Berendsen temperature coupling method. Parrinello-Rahman pressure coupling method was utilized in NPT equilibration. The final production step of molecular dynamics simulation was carried out for 50 ns, each step of 2 fs. Trajectories were saved, and results were analyzed using XMGRACE. Root mean square deviation (RMSD) variation in protein backbone was calculated by using g RMS tool, which utilizes the least-square fitting method. Overall root mean square fluctuation (RMSF) in the atomic positions of protein C backbone was calculated by using the g rmsf tool. A rough measure of the compactness factor of protein during the course of the simulation was estimated by using the g gyrate tool of GROMACS. Gmxsasa was used for

computation of the total solvent accessible surface area (SASA). Hydrogen bonds were calculated with 3.5Å distance cut-off by using g h bond, and the distribution of intermolecular hydrogen bond lengths throughout the simulation was also analyzed.

2.6 MM/G/P/BSA binding Free Energy Calculations

Molecular Mechanic/Poisson-Boltzmann Surface Area (MMPBSA) method was used to obtain the binding free energy of the interaction between ligand-protein complexes (Aldeghi et al., 2017). This employs ensembles derived from MD simulation. The g mmpbsa application of GROMACS module was used for the calculation of different components of the binding free energy of the M^{pro} and ligand complexes. Here, the binding energy is an average of three energetic terms, *i.e.* potential energy in the vacuum, polar-solvation energy, and non-polar solvation energy, respectively. The snapshots at every 100ps between 40 and 50 ns were collected, and MMPBSA was performed to predict the binding energy.

In the MMPBSA calculation, the binding free energy between a receptor and a ligand was calculated using following equations:

$$\Delta G_{MMPBSA} = G_{complex} - G_{protein} - G_{ligand}\ complex \quad (1)$$

$$G_x = E_{MM} - T S_{MM} + \Delta G_{solv} \quad (2)$$

$$E_{MM} = E_{bonded} + E_{coul} + E_{LJ} \quad (3)$$

$$\Delta G_{solv} = G_{polar} + G_{nonpolar} \quad (4)$$

2.7 Computational Facility Details

The MD simulations and corresponding energy calculations were carried out on HP Gen7 server with 48 Core AMD processors and 32GB of RAM.

3. Results And Discussion

3.1 Molecular Docking

The molecular docking approach to identify the drug targets has become one of the most popular methods for ligand-based computer-aided drug discovery (LB-CADD). In current era, with this approach, big data of drug libraries can be analyzed and annotated quickly and immense amount of energy, time, and costs related to CADD can be saved (Wadood et al., 2013; Yu & Mackerell, 2017). Currently, there are no effective treatments available to cure COVID-19 virus, and hence, identification of potential drug targets is urgently needed.

We used molecular modeling approach with molecular docking and MD simulation to identify potential phytochemcials active against the M^{pro} protein of COVID-19. These screened natural compounds may pave way for the development of drugs against COVID-19. On the basis of AutoDock binding affinity, phytochemicals namely, carvacrol, oleanolic acid and ursolic acid have shown satisfactory interactions with active site residues. These compounds have been found to have binding energy of -4.0 kcal/mol, -6.0 kcal/mol, -5.9 kcal/mol, respectively. The docked ligand molecules with protease are shown in **Figure 2**. **Table 1** represented the 2D and 3D structures of docked ligand molecules along with AutoDock score. Hydrogen bonds play an important role in determining its specificity and affinity within protein-ligand complexes (Sakkiah et al., 2012).

In order to evaluate the affinity of the ligand molecules with the M^{pro} protein, we also studied the residues of protease involved in forming hydrogen bonds with the phytochemicals and the strength of these bonds. Amino acids residues participated in hydrophobic interactions between protease and ligand molecules were also investigated. Molecular interactions (hydrogen bonds and hydrophobic interactions) play a key role in giving shape and stabilizing the docking complexes (Wade & Goodford, 1989).

With AutoDock binding energy -4.0 kcal/mol, Gly143 amino acid was found to be involved in forming hydrogen bond with carvacrol (**Figure 2**). In addition to this, six other residues (Leu27, His41, Met49, Asn142, Cys145, Met165) are involved in forming hydrophobic interactions**.** Oleanolic acid compound make complex using AutoDock with binding energy -6.0 kcal/mol. The Gln189 amino acid formed the hydrogen bond**,** and two amino acids (Cys145, His163) were involved in hydrophobic interactions. Autodock binding energy of ursolic acid compound was -5.9 kcal/mol. The Ser46 amino acid at the active site of protease formed hydrogen bond. Nine amino acids (Thr24, Thr25, Thr26, Cys44, Thr45, Asn142, Gly143, Cys145, Glu166) participated in the formation of van der Waals interactions **(Figure 2).** Carvacrol having less binding energy as compared to oleanolic acid and ursolic acid molecules, the binding mode of interaction was found to be reasonably good. Previous studies reported a similar trend of the presence of binding pockets in main M^{pro} of SARS-CoV, which confirms our study (Li et al., 2020; Muralidharan et al., 2020; Khan et al., 2020; Aanouz et al., 2020). Aanouz et al., 2020 reported the β–Eudesmol molecule as a potential inhibitor of M^{pro} of COVID-19 based on its significant antibacterial and antiviral power well documented in literatures. However, this compound showed the low affinity interaction with M^{pro} and formed the hydrogen only with Thr111.

In our earlier study we have reported the ursolic acid carvacrol molecules as potential inhibitors of Small heat shock protein16.3 (sHSP16.3) of *Mycobacterium tuberculosis* (MTB) (Jee et al., 2018). Docking study of ursolic acid with sHSP16.3 formed two strong hydrogen bonds with Glu56 and Pro58, while carvacrol was found to be bound with only one hydrogen bond Glu92. Binding affinity of both compounds with sHSP16.3 confirms the present study results. From a biological point of view, reported phytochemicals, carvacrol, oleanolic acid and ursolic acid which are proposed as potential inhibitors of the M^{pro} having a significant antiviral activity with evident to bibliographical research and performed *in-vitro* studies (Gilling et al., 2014; Jesus et al., 2015; Khwaza et al., 2018; Kamalabadi et al., 2018; Tohmé et al., 2019; Marinelli et al., 2019).

Table 1. Molecular docking results of carvacrol, oleanolic acid and ursolic acid.

Compound Name	PubChem ID	Chemical Structure		Docking Energy (AutoDock)
		2D	3D	
Carvacrol	CID_10364		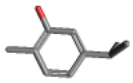	-4.0 kcal/mol
Oleanolic acid	CID_10494	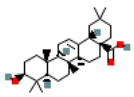	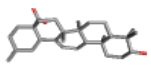	-6.0 kcal/mol
Ursolic acid	CID_64945	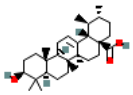		-5.9 kcal/mol

3.2. Evaluation of Drug Likeness

Carvacrol, oleanolic acid and ursolic acid have respectively the following molecular weights (150.22, 456.70, 456.70) g/mol, all three molecules have molecular weight ≤ 500 g,/mol which follows the Lipinski's rule. The carvacrol molecule has been found to have topological polar surface (TPSA) as 20.23 Å², while oleanolic acid and ursolic acid molecules were found to have 57.53 Å². According to the rule lowest TPSA values always produce good results; therefore, we noted that selected molecules are better behaved than the co-crystallized ligand (Lipinski et al., 2001; Daina et al., 2017). The (LogP) values of carvacrol, oleanolic acid and ursolic acid were found with the range of 2.82, 6.06, 5.94, respectively. Predicted LogP values depict that these molecules can be absorbed in the body. All three molecules present number of hydrogen bond donors: ≤5, a number of hydrogen bond acceptors ≤10 and also molar refractivity values between 48.01, 136.65, 136.91, respectively. The hydrogen bonding and molar refractivity calculations showed that these molecules validate the five Lipinski's rule. These molecules also follow the Veber's rule which denotes the oral bioavailability of drug molecules. Since in some CAD molecules cannot be synthesized, synthetic accessibility (SA) is a key aspect of drug designing. The carvacrol, oleanolic acid and ursolic acid molecules were found to have SA score 1, 6.08, 6.21, respectively. According to SA method molecules having score 1 is easy to synthesize it, on the other hand, score 10 represent difficulties to synthesize the molecules. All three molecules having less than 10 score, so they can be easily synthesized. The results of the ADME calculations are listed in the **Table 2**.

Table 2. List of the results of the phytochemical molecules druglikeness properties

Drug Likeness Properties	Carvacrol	Oleanolic acid	Ursolic acid
Molecular weight g/mol	150.22	456.70	456.70
Concensus Log Po/w	2.82	6.06	5.94
Num. H-bond acceptors	1	3	3
Num. H-bond donors	1	2	2
Molar Refractivity	48.01	136.65	136.91
Lipinski	Yes	Yes	Yes
Veber	Yes	Yes	Yes
Bioavailability score	0.55	0.56	0.56
Synthetic accessibility (SA)	1.00	6.08	6.21
TPSA (Å)	20.23	57.53	57.53
No of rotatable bonds	1	1	1
Solubility	1.46e-01	3.45e-04	9.72e-04

3.2 MD Simulations

MD simulations are one of proven *in-silico* methods for obtaining dynamic data at atomic spatial resolution and picoseconds or finer temporal resolution (Benson & Daggett, 2012; Gajula et al., 2016). The main protease docked complexes with phytochemical compounds; carvacrol, ursolic acid and oleanolic acid simulation study done for 50 ns simulation period to analyze the stability of these docked phytochemical compounds in binding region of M^{pro}.

The M^{pro} with compound carvacrol (black) showed stable and constant range of RMSD between 0.23nm to 0.30nm and similar results showed by ursolic acid (blue), only slight changes showed in starting of the simulation. The oleanolic acid (red) showed stable RMSD between 4ns to 20ns at RMSD range between 0.21nm to 0.38nm, after 20ns RMSD increases and constant at 0.41nm (**Figure 3**). The differences of backbone RMSD with carvacrol, ursolic acid and oleanolic acid complex in protein backbone RMSD suggest that M^{pro} have conformational changes in oleanolic acid while no significant change shown in carvacrol and ursolic acid during 50ns simulation.

The compound carvacrol (red) has shown fluctuations at two different intervals on 50 ns time scale as it may has changed a conformation in binding region of M^{pro}. The first stable conformation between 6ns to 29ns and second stable conformation is between 34ns to 50ns. The RMSD remain constant at 0.3nm and large fluctuation observed between 28ns to 33ns RMSD>0.4nm. As large fluctuation in compound, no effect on protein structure was found. Similar changes also seen in ursolic acid (magenta) RMSD fluctuations, it shown stable RMSD after 18ns between 0.58nm to 0.66nm while in starting period between 4ns to 17ns, RMSD consistently fluctuated (**Figure 4**). It also not affects the fluctuation of protein backbone which depicts that binding region of protein has some fluctuation that causes the compound fluctuations during simulation. It may cause by large binding region and presence of loop at binding region.

The oleanolic acid (blue) showed higher but stable RMSD between 0.44nm to 0.61nm throughout simulation. Oleanolic acid binding affects the RMSD of protein backbone but it has stable till end of the simulation. Two similar conformations of ursolic and oleanolic acid molecules showed different behaviour with protein binding region during simulation analysis. This observation we also confirm by their local changes in residues level by RMSF plot. Protein backbone with carvacrol (black) and ursolic acid (blue) not affect the behaviour of protein or structure of protein during simulation while oleanolic acid (red) affects the structure of protein during simulation. RMSF confirms the changes in structure with binding of these phytochemical compounds (**Figure 5**).

3.3 Hydrogen Bond Analysis

Hydrogen bonding plays a crucial role in determining the binding strength in between ligands and protein. The carvacrol (red) and ursolic acid (black) have constant range of hydrogen bond between 2 to 4 in whole simulation while oleanolic acid showed changes in bonding. More hydrogen (>5) bonds between 0 to 12ns, after 12ns the hydrogen bond are <4 and last 10ns, the hydrogen bond between 2 to 3. This may suggests that there is a conformational change around oleanolic acid in the binding site during simulation (**Figure 6**). Over all observation suggested that all three protein-ligand complexes are stable during simulation.

3.4 Free Binding Energy Analysis/Poisson–Boltzmann Surface Area (MM-PBSA)

The pre docking suggest the binding energy of complex while binding free energy (ΔG bind) analysis after simulation suggest the consistency of non-bonding interactions energy of binding region with compound also called post docking. In previous reports, it has been shown that 100-200 snapshots are enough to calculate the binding free energies (Khan et al. 2020; Khan et al., 2020; Sarma et al., 2020). The van der waal energy component compared with each complex, the carvacrol (-93.913 +/-9.776) has less effect on binding affinity while ursolic (-189.889 +/-12.027) and oleanolic acid (-197.509 +/-11.086) has strong binding affinity. Similar results are shown in binding energy, ursolic (-168.918 +/-13.703) and oleanolic acid (-158.999 +/-15.306) showed similar effect of binding energy while moderate in carvacrol (-82.781 +/- 9.401). The electrostatic energy doesn't show significant in ursolic and oleanolic acid while moderate in carvacrol. The polar solvation and SASA energy are shown moderate effects on binding energy component in each compound (**Table 3**).

Table 3. Free binding energy calculations of each M^{pro} and ligand complexes.

Complexes	Binding energy (kJ/mol)	van der Waal energy (ΔEvdW) (kJ/mol)	Electrostattic energy (ΔEelec), (kJ/mol)	Polar solvation energy (ΔG polar) (kJ/mol)	SASA energy (kJ/mol)
Carvacrol	-82.781 +/- 9.401	-93.913 +/-9.776	-37.778 +/- 6.738	58.079 +/- 6.712	-9.169 +/- 0.708
Oleanolic acid	-158.999 +/-15.306	-197.509 +/-11.086	-5.129 +/- 5.617	59.634 +/- 8.719	-15.995 +/- 0.944
Ursolic acid	-168.918 +/-13.703	-189.889 +/-12.027	-1.985 +/- 2.485	37.781 +/- 9.198	-14.825 +/- 1.721

3.5 Radius of gyration Analysis

In order to determine the compactness of the system with the time, Rg was calculated, in which higher Rg values depict less compactness (more unfolded) with conformational entropy, while low Rg values explain high compactness with more stability in the structure (more folded). As evident from **Figure 7a**, the simulation Rg values of all three cases reported as 2.05-2.15 nm. The fewer changes in the Rg value exhibited the stability of the protein in the complex, which showed less difference. Rg results revealed that the binding of these three molecules does not induce structural changes. The Rg values of all three protein-ligand complexes (**Figure 7a**) support their condensed architecture as well as size. In a recent study, Khan et al. (2020) calculated the Rg values for Remdesivir Saquinavir and Darunavir drugs (reported as inhibiting drugs against chymotrypsin-like protease of SARS-CoV-2). The average gyration score of Remdesivir was found to be 22.25 ± 0.1 Å, while Saquinavir and Darunavir durgs prompted to have average Rg scores of 22.32 ± 0.4 Å and 22.29 ± 0.6 Å, respectively.

3.6 SASA Analysis

Additionally, we also conducted the solvent accessible surface area (SASA) analysis of all of the three protein-ligand complexes. SASA is important to measure of the receptor exposed to the solvents during the simulation. The exposures of the hydrophobic residues by the binding of the ligand molecules contribute to the values of the SASA. The SASA value exhibited between 155-165 nm^2 (**Figure 7b**) showed that the binding of ligands does not affect the folding of the protein. Khan et al. (2020) have performed the SASA analysis for $3CL^{pro}$ and its protein-drug complexes. They reported that SASA values for the $3CL^{pro}$, $3CL^{pro}$-Paritaprevir complex and $3CL^{pro}$-Raltegravir complex were 133.89 nm^2, 131.79 nm^2 and 131.26 nm^2, respectively. The results reported in the present study suggest that all three of the complexes were impressively stable after the binding of ligands to active sites of M^{pro} protein.

4. Conclusion

The M^{pro} protein has shown to be crucial and highly potent target for the inhibition of novel COVID-19. This study concludes three natural compounds (ursolic acid, carvacrol and oleanolic acid) as potential inhibitors against M^{pro}. Molecular docking analysis revealed that Carvacrol molecule having less binding energy as compared to other two molecules, oleanolic acid and ursolic acid. The binding mode of interaction was found to be reasonably good. MD simulations revealed that all three docking complexes showed stability at 50ns. These inhibitors also fulfil the ADME parameters as well as Lipinski's rule of five. All these reported compounds are natural and also commercially available for further *in vivo/in vitro* validations. The information generated from this present study may be utilized in future for the development of more phytochemical based therapeutics against COVID-19.

Abbreviations

SARS-CoV-2: Severe acute respiratory syndrome coronavirus-2, COVID-19: Corona virus disease 2019, MD: Molecular dynamic, Mpro: protease, MM/G/P/BSA: Molecular mechanic/generalized/Born/Poisson-Boltzmann surface area, CSG: Coronavirus study group, ICTV: International committee on taxonomy of viruses, WHO: World health organization, ORFs: Open reading frames, RTC: Replicase/ transcriptase complex, PDB: Protein data bank, ADME: Absorption, Distribution, Metabolism, and Excretion, RMSD: Root mean square deviation, RMSF: Root mean square fluctuation, SASA: Solvent accessible surface area, LB-CADD: Ligand-based computer-aided drug discovery, Rg: Radius of gyration

Declarations

Conflict of interest

The authors declare that the research was conducted in the absence of any commercial or financial relationships that could be construed as a potential conflict of interest.

Ethical standards

Ethical standards are compulsory for studies relating to human and animal subjects.

Acknowledgement

Authors are thankful to Dr. Prashanth N Suravajhala, Birla Institute of Scientific Research (BISR). Jaipur, Rajasthan and Dr. MNV Prasad Gajula, Institute of Biotechnology, Hyderabad for critical proofreading of final manuscript. AK thanks the Director, UCB for encouragement, suggestions and timely help.

References

Aanouz, I., Belhassan, A., El Khatabi, K., Lakhlifi, T., El Idrissi, M., & Bouachrine, M. (2020). Moroccan medicinal plants as inhibitors of COVID-19: Computational investigations. *Journal of Biomolecular Structure and Dynamics*. https://doi.org/10.1080/07391102.2020.1758790

Abdelli, I., Hassani, F., Brikci, & S.B., Said. (2020). In silico study the inhibition of Angiotensin converting enzyme 2 receptor of COVID-19 by Ammoidesverticillata components harvested from western Algeria. *Journal of Biomolecular Structure and Dynamics*. https://doi.org/10.1080/07391102.2020.1763199

Adem, S., Eyupoglu, V., Sarfraz, I., Rasul, A., & Ali, M. (2020). Identification of potent COVID–19 main protease (Mpro) inhibitors from natural polyphenols: an in silico strategy unveils a hope against CORONA. *Preprints*, 2020030333. doi: 10.20944/preprints202003.0333.v1

Aldeghi, M., Bodkin, M.J., Knapp, S., & Biggin, P.C. (2017).
Statistical analysis onthe performance of molecular mechanics poissonboltzmann surface area versus absolute binding free energy calculations: bromodoma a case study. *Journal of Chemical Information and Modeling, 57*(9), 2203-2221.

Anand, K., Ziebuhr, J., Wadhwani, P., Mesters, J.R., & Hilgenfeld, R. (2003). Coronavirus main proteinase (3CLpro) structure: basis for design of anti-SARS drugs. *Science, 300*, 1763-1767.

Anand, K., Yang, H., Bartlam, M., Rao, Z., & R. Hilgenfeld. (2005). Coronavirus main proteinase: Target for antiviral drug therapy. In A. Schmidt, O. Weber, & M. H. Wolff (Eds.), *Coronaviruses with special emphasis on first insights concerning SARS* (pp. 173–199). Birkhäuser Basel. 10.1007/3-7643-7339-3_9.

Benson, N.C., & Daggett, V. (2012). A comparison of multiscale methods for the analysis of molecular dynamics simulations. *The Journal of Physical Chemistry B, 116*(29), 8722-8731.

Berendsen, H.J.C., van der Spoel, D., & van Drunen, R. (1995). GROMACS: a message-passing parallel molecular dynamics implementation. Computer *Physics Communications, 91*(1-3), 43-56.

Berman, H.M., Westbrook, J., Feng, Z., Gilliland, G., Bhat, T.N., Weissig, H., Shindyalov, I.N., & Bourne, P.E. (2000). The protein data bank. *Nucleic Acids Research*, ***28***, 235-242. doi:10.1093/nar/28.1.235

Bhatraju, P.K., Ghassemieh, B.J., Nichols, M., Kim, R., Jerome, K.R., Nalla, A.K., Greninger, A.L., Pipavath, S., Wurfel, M.M., Evans, L., Kritek, P.A., West, T.E., Luks, A., Gerbino, A., Dale, C.R., Goldman, J.D., O'Mahony, S., & Mikacenic, C. (2020). *The New England Journal of Medicine*. doi: 10.1056/NEJMoa2004500

Boopathi, S., Poma, A.B., & Kolandaivel, P. (2020). Novel 2019 coronavirus structure, mechanism of action, antiviral drug promises and rule out against its treatment. *Journal of Biomolecular Structure and Dynamics*. https://doi.org/10.1080/07391102.2020.1758788

Burley, S. K., Berman, H. M., Bhikadiya, C., Bi, C., Chen, L., Di Costanzo, L., & Feng, Z. (2019). RCSB Protein Data Bank: biological macromolecular structures enabling research and education in fundamental biology, biomedicine, biotechnology and energy. *Nucleic Acids Research, 47*(D1), 464-474.

Chan, J.F.-W., Yuan, S., Kok, et al. (2020). A familial cluster of pneumonia associated with the 2019 novel coronavirus indicating person-to-person transmission: A study of a family cluster. *The Lancet*, *395*(10223), 514–523. doi:10.1016/S0140-6736(20)30154-9

Chandel, V., Raj, S., Rathi, B., & Kumar, D. (2020). *In silico* identification of potent COVID–19 main protease inhibitors from FDA approved antiviral compounds and active phytochemicals through molecular docking: a drug repurposing approach. *Preprints,* 2020030349.

Chang, C., Lo, S.-C., Wang, Y.-S., & Hou, M.-H. (2016). Recent insights into the development of therapeutics against coronavirus diseases by targeting N protein. *Drug Discovery Today*, *21*(4), 562–572.

Chang, Y., Tung, Y., Lee, K., Chen, T., Hsiao, Y., Chang, H & Shih, S. (2020). Potential therapeutic agents for COVID–19 based on the analysis of protease and RNA polymerase docking. *Priprints,* 2020020242. doi: 10.20944/preprints202002.0242.v1

Chen, Y., Liu, Q., & Guo, D. (2020). Emerging coronaviruses: Genome structure, replication, and pathogenesis. *Journal of Medical Virology*, *92*(4), 418–423.

Contini, A. (2020): Virtual screening of an FDA approved drugs database on two COVID-19 coronavirus proteins. *ChemRxiv. Preprint*. doi: doi.org/10.26434/chemrxiv.11847381.v1

Coronaviridae Study Group of the International Committee on Taxonomy of Viruses. (2020). The species severe acute respiratory syndrome-related coronavirus: Classifying 2019-nCoV and naming it SARS-CoV-2. *Nature Microbiology*, 1. 10.1038/s41564-020-0695-z.

Daina A, Michielin O, Zoete V (2017) SwissADME: a free web tool to evaluate pharmacokinetics, drug-likeness and medicinal chemistry friendliness of small molecules. Sci Rep 7:42717. https://doi.org/10.1038/srep42717

Das, S., Sarmah, S., Lyndem, S., & Roy, A.S. (2020). An investigation into the identification of potential inhibitors of SARS-CoV-2 main protease using molecular docking study. *Journal of Biomolecular Structure and Dynamics*. https://doi.org/10.1080/07391102.2020.1763201

de Wit, van Doremalen, N., Falzarano, D., & Munster, V. J. (2016). SARS and MERS: Recent insights into emerging coronaviruses. *Nature Reviews Microbiology*, *14*(8), 523–534.

Devaux, C., Rolain, J., Colson, P &Raoult, D. (2020). New insights on the antiviral effects of chloroquine against coronavirus: what to expect for COVID–19?.*International Journal of Antimicrobial Agents, 105938.*

Elfiky A.A. (2020a). SARS-CoV-2 RNA dependent RNA polymerase (RdRp) targeting: An in-silico perspective. *Journal of Biomolecular Structure and Dynamics*. https://doi.org/10.1080/07391102.2020.1761882

Elfiky A.A. (2020b). Natural products may interfere with SARS-CoV-2attachment to the host cell. *Journal of Biomolecular Structure and Dynamics*. https://doi.org/10.1080/07391102.2020.17618

Elfiky, A.A., & Azzam, E.B. (2020). Novel guanosine derivatives against MERS CoV polymerase: An in-silico perspective, *Journal of Biomolecular Structure and Dynamics*. https://doi.org/10.1080/07391102.2020.1758789

Elmezayen, A.D., Al-Obaidi, A., Şahin, A.T., & Yelekci, K. (2020). Drug repurposing for coronavirus (COVID-19): in silicoscreening of knowndrugs against coronavirus 3CL hydrolase and protease enzymes. *Journal of Biomolecular Structure and Dynamics*. https://doi.org/10.1080/07391102.2020.1758791

Enayatkhani, M., Hasaniazad, M., Faezi, S., Guklani, H., Davoodian, P., Ahmadi, N., Einakian, M.A., Karmostaji, A., & Ahmadi, K. (2020). Reverse vaccinology approach to design a novel multi-epitope vaccine candidate against COVID-19: an in silico study. *Journal of Biomolecular Structure and Dynamics*. https://doi.org/10.1080/07391102.2020.1756411

Enmozhi, S.K., Raja, K., Sebastine, I., & Joseph, J. (2020). Andrographolide as a potential inhibitor of SARS-CoV-2 main protease: an in-silico approach. *Journal of Biomolecular Structure and Dynamics*. https://doi.org/10.1080/07391102.2020.1760136

Gajula, M.N.P. (2008). Computer simulation meets experiment: molecular dynamics simulations of spin labeled proteins
MNV Prasad Gajula, PhD dissertation 2008/3/18; urn:nbn:de:gbv: 700-2008041631 Universität Osnabrück

Gajula, M.N.P., Kumar, A., & Ijaq, J. (2016). Protocol for molecular dynamics simulations of proteins. *Bio-protocol, 6*, 1-11. doi:10.21769/BioProtoc.2051

Gentile, D., Patamia, V., Scala, A., Sciortino, M. T., Piperno, A., & Rescifina, A. (2020). Inhibitors of SARS-CoV–2 main protease from a library of marine natural products: a virtual screening and molecular modeling study. *Preprints,* 2020030372.

Gilling, D.H., Kitajima, M., Torrey, J.R., & Bright, K.R. (2014). Antiviral efficacy and mechanisms of action of oregano essential oil and its primary component carvacrol against murine norovirus. *Journal of Applied Microbiology, 116*(5), 1149-1163.

Gonzalez-Paz, L.A., Lossada, C.A., Moncayo, L.S., Romero, F., Paz, J.L., Vera-Villalobos, J., Pérez, A.E., San-Blas, E., Alvarado, Y.J. (2020). Theoretical molecular docking study of the structural disruption of the viral 3CL-protease of COVID19 induced by binding of capsaicin, piperine and curcumin part 1: a comparative study with chloroquine and hydrochloroquine two antimalaric drugs. *Research Square,* (preprint). doi: 10.21203/rs.3.rs-21206/v1

Gorden, D.E., Gwendolyn, M.J., Bouhaddou, M., et al. (2020). A SARS-CoV-2-human protein-protein interaction map reveals drug targets and potential drug-repurposing. *bioRxiv*. https://doi.org/10.1101/2020.03.22.002386

Gupta, M.K., Vemula, S., Donde, R., Gouda, G., Behera, L., & Vadde, R. (2020). *In-silico* approaches to detect inhibitors of the human severe acute respiratory syndrome coronavirus envelope protein ion channel. *Journal of Biomolecular Structure and Dynamics*. https://doi.org/10.1080/07391102.2020.1751300

Hasan, A., Paray, B.A., Hussain, A., Qadir, F.A., Attar, F., Aziz, F.M., Sharifi, M., Derakhshankhah, H., Rasti, B., Mehrabi, M., Shahpasand, K., Saboury, A.A., & Falahati, M. (2020). A review on the cleavage priming of the spike protein on coronavirus by angiotensin-converting enzyme-2 and furin. *Journal of Biomolecular Structure and Dynamics*. https://doi.org/10.1080/07391102.2020.1754293

Hemida, M. G., & Ba Abduallah, M. M. (2020). The SARS-CoV-2 outbreak from a one health perspective. *One Health*, 100127.

Hyldgaard, M., Mygind, T., & Meyer, R. L. (2012). Essential oils in food preservation: mode of action, synergies, and interactions with food matrix components. *Frontiers in Microbiology, 3*, 12. doi: 10.3389/fmicb.2012.00012

Islam, R., Parves, R., Paul, A.S.,Uddin, N., Rahman, M.S., Mamun, A.A., Hossain, M.N., Ali, M.A., & Halim, M.A. (2020). A molecular modeling approach to identify effective antiviral phytochemicals against the main protease of SARS-CoV-2. *Journal of Biomolecular Structure and Dynamics.* https://doi.org/10.1080/07391102.2020.1761883

Jee, B., Kumar, S., Yadav, R., Singh, Y., Kumar, A., & Sharma, M. (2018). Ursolic acid and carvacrol may be potential inhibitors of dormancy protein small heat shock protein16.3 of *Mycobacterium tuberculosis*, *Journal of Biolomolecular Structure and Dynamics, 36*(13), 3434-3443.

Jesus, J.A., G. Lago, J.H., Laurenti, M.D., Yamamoto, E.S., & D. Passero, L.F. (2015). Antimicrobial activity of oleanolic and ursolic acids: an update. *Evidence-Based Complementary and Alternative Medicine, 2015*, 620472. doi: https://doi.org/10.1155/2015/620472

Jin, Z., Du, X., Xu, Y., Deng, Y., Liu, M., Zhao, Y., & Zhang, B. (2020). Structure of Mpro from COVID-19 virus and discovery of itsinhibitors. *bioRxiv*. https://www.biorxiv.org/content/10.1101/2020.02.26.964882v2

Joshi, R.S., Jagdale, S.S., Bansode, S.B., Shankar, S.S., Tellis, M.B., Pandya, V.K., Chugh, A., Giri, A.P., & Kulkarni, M.J. (2020). Discovery of potential multi-target-directed ligands by targeting host-specific SARS-CoV-2 structurally conserved main protease, *Journal of Biomolecular Structure and Dynamics*. https://doi.org/10.1080/07391102.2020.1760137

Kaisari, E., & Borruat, F. (2020). Keeping an eye on hydroxychloroquine retinopathy. *KlinischeMonatsblätterfürAugenheilkunde*. Efirst.

Kamalabadi, M., Astani, A., & Nemati, F. (2018). Anti-viral effect and mechanism of carvacrol on herpes simplex virus type 1. *International Journal of Molecular Laboratory, 5*(2), 113-122.

Khaerunnisa, S., Kurniawan, H., Awaluddin, R., Suhartati, S., & Soetjipto, S. (2020). Potential inhibitor of COVID–19 main protease (M^{pro}) from several medicinal plant compounds by molecular docking study. *Preprints,* 2020030226.

Khan, S.A., Zia, K., Ashraf, S., Uddin, R., & Ul-Haq, Z. (2020). Identification of chymotrypsin-like protease inhibitors of SARS-CoV-2 via integrated computational approach. *Journal of Biomolecular Structure and Dynamics*, 1-10. doi: 10.1080/07391102.2020.1751298.

Khwaza, V., Oyedeji, O.O., & Aderibigbe, B.A. (2018). Antiviral activities of oleanolic acid and its analogues. *Molecules, 23*(9), 2300. doi: 10.3390/molecules23092300

Kim, S., Chen, J., Cheng, T., Gindulyte, A., He, J., He, S., Li, Q., Shoemaker, B.A., Thiessen, P.A., Yu, B., Zaslavsky, L., Zhang, J., &Bolten, E.E. (2019). PubChem 2019 update: improved accesses to chemical data. *Nucleic Acids Research, 47*(D1), 1102-1109. doi: 10.1093/nar/gky1033.

Kumar, A., Kumar, R., Sharma, M., Kumar, U., Gajula, M.NV.P., & Singh, K.P. (2018). Uttarakhand medicinal plants database (UMPDB): a platform for exploring genomic, chemical, and traditional knowledge. *Data (MDPI), 3*(1), 7. doi: 10.3390/data3010007

Kumar, A., Kumar, S., Kumar, A., Sharma, N., Sharma, M., Singh, K.P., Rathore, M., & Gajula, M.N.V.P. (2018). Homology modeling, molecular docking and molecular dynamics based functional insights into rice urease bound to urea. *Proceedings of the National Academy of Sciences, India Section B: Biological Sciences, 88*, 1539–1548.

Li, Y., Zhang, J., Wang, N., Li, H., Shi, Y., Guo, G., & Zou, Q. (2020). Therapeutic drugs targeting 2019-nCoV main protease by high-throughput screening. *bioRxiv*. doi:10.1101/2020.01.28.922922

Lipinski, C. A., Lombardo, F., Dominy, B. W., Feeney, P. J. 2001. Experimental and computational approaches to estimate solubility and permeability in drug discovery and development settings. *Advances in Drug Delivery Reviews*, 46, 3-26.

Lu, I.-L., Mahindroo, N., Liang, P.-H., Peng, Y.-H., Kuo, C.-J., Tsai, K.-C., Hsieh, H.-P., Chao, Y.-S., & Wu, S.-Y. (2006). Structure-based drug design and structural biology study of novel nonpeptide inhibitors of severe acute respiratory syndrome coronavirus main protease. *Journal of Medicinal Chemistry*, *49*(17), 5154–5161.

Mackenzie, J.S., & Smith, D.W. (2020). COVID-19: a novel zoonotic disease caused by a coronavirus from China: what we know and what we don't. *Microbiology Australia, MA20013*.doi: 10.1071/MA20013

Marinelli, L., Fornasari, E., Eusepi, P., Ciulla, M., Genovese, S., Epifano, F., & Cacciatore, I. (2019). Carvacrol prodrugs as antimicrobial agents. *European Journal of Medicinal Chemistry, 178*, 515–529. doi: 10.1016/j.ejmech.2019.05.093.

Morris, G. M., Huey, R., Lindstrom, W., Sanner, M. F., Belew, R. K., Goodsell, D. S., & Olson, A. J. (2009). Autodock4 and AutoDockTools4: automated docking with selective receptor flexiblity. *Journal of Computational Chemistry*, **16**, 2785-91.

Muralidharan, N., Sakthivel, R., Velmurugan, D., & Gromiha, M.M. (2020). Computational studies of drug repurposing and synergism of lopinavir, oseltamivir and ritonavir binding with SARS-CoV-2 protease against COVID-19. *Journal of Biomolecular Structure and Dynamics*. https://doi.org/10.1080/07391102.2020.1752802

Panchangam, S.S., Vahedi, M., Megha, M.J., Kumar, A., Raithatha, K., Suravajhala, P., & Reddy, P. (2016). Saffron'omics': The challenges of integrating omic technologies. *Avicenna Journal of Phytomedicine, 6*, 604–620.

Pant, S., Singh, M., Ravichandiran, V., Murty, U.S.N., Srivastava, & H.K.. (2020). Peptide-like and small-molecule inhibitors against Covid-19. *Journal of Biomolecular Structure and Dynamics*. https://doi.org/10.1080/07391102.2020.1757510

Pollier, J., & Goossens, A. (2012). Oleanolic acid. *Phytochemistry, 77*, 10-15.

Qamar, M., Alqahtani, S., Alamri, M., & Chen, L. (2020). Structural basis of SARS-CoV–2 3CLpro and anti-COVID–19 drug discovery from medicinal plants. *Journal of Pharmaceutical Analysis.* Doi: https://doi.org/10.1016/j.jpha.2020.03.009

Sakkiah, S., Chandrasekaran, M., Lee, .Y, Kim, S., & Lee, K.W. (2012). Molecular modeling study for conformational changes of Sirtuin 2 due to substrate and inhibitor binding. *Journal of Biomolecular Structure and Dynamics, 30*(3), 235-254.

Salata, C., Calistri, A., Parolin, C., & Palù, G. (2019). Coronaviruses: A paradigm of new emerging zoonotic diseases. *Pathogens and Disease*, *77*(9), ftaa006.

Sarma, P., Sekhar, N., Prajapat, M., Avti, P., Kaur, H., Kumar, S., Singh, S., Kumar, H., Prakash, A., Dhibar, D.P., & Medhi, B. (2020). *In-silico* homology assisted identification of inhibitor of RNA binding against 2019-nCoV N-protein (N terminal domain). *Journal of Biomolecular Structure and Dynamics*. https://doi.org/10.1080/07391102.2020.1753580

Schüttelkopf, A.W., & van Aalten, D. M. F. (2004). PRODRG: a tool for high-throughput crystallography of protein-ligand complexes. *Acta Crystallographica*, *60*, 1355–1363.

Seah, I., & Agrawal, R. (2020). Can the coronavirus disease 2019 (COVID-19) affect the eyes? A review of coronaviruses and ocular implications in humans and animals. *Ocular Immunology and Inflammation*, 1–5.

Sharma, A.D., & Kaur, I. (2020). Eucalyptol (1,8 cineole) from eucalyptus essential Oil a potential inhibitor of COVID 19 corona virus infection by molecular docking studies. *Preprints*, 2020030455.

Sinha, S.K., Shakya, A., Prasad, S.K., Singh, S., Gurav, N.S., Prasad, R.S., & Gurav, S.S. (2020). An in-silico evaluation of different Saikosaponins for their potency against SARS-CoV-2 using NSP15 and fusion spike glycoprotein as targets. *Journal of Biomolecular Structure and Dynamics*. https://doi.org/10.1080/07391102.2020.1762741

Su, S., Wong, G., Shi, W., Liu, J., Lai, A. C. K., Zhou, J., Liu, W., Bi, Y., & Gao, G. F. (2016). Epidemiology, genetic recombination, and pathogenesis of coronaviruses. *Trends in Microbiology*, *24*(6), 490–502.

Sun, N., Wong, W., & Guo, J. (2020). Prediction of potential 3CLpro-targeting anti-SARS-CoV–2 compounds from Chinese medicine. *Preprints,* 2020030247.

Tohmé, M.J., Giménez, M.C., Peralta, A., Colombo, M.I., & Delgui, L.R. (2019). Ursolic acid: A novel antiviral compound inhibiting rotavirus infection in vitro. *International Journal of Antimicrobial Agents, 54*(5), 601-609.

Umesh, Kundu, D., Selvaraj, C., Singh, S.K., & Dubey, V.K. (2020). Identification of new anti-nCoV drug chemical compounds from Indian spices exploiting SARS-CoV-2 main protease as target. *Journal of Biomolecular Structure and Dynamics*. https://doi.org/10.1080/07391102.2020.1763202

Veber, D. F., Johnson, S. R., Cheng, H. Y., Smith, B. R., Ward, K. W., & Kopple, K. D. 2002. Molecular properties that influence the oral bioavailability of drug candidates. Journal of medicinal chemistry, 45(12), 2615-2623.

Wade, R.C., & Goodford, P.J. (1989). The role of hydrogen-bonds in drug binding. *Progress in Clinical and Biological Research, 289*, 433-444.

Wadood, A., Ahmed, N., Shah, L., Ahmad, A., Hassan, H., & Shams, S. (2013). In-silico drug design: An approach which revolutionarised the drug discovery process. *OA Drug Design & Delivery, 1*(1), 3.

Wahedi, H.M., Ahmad, S., & Abbasi, S.W. (2020). Stilbene-based natural compounds as promising drug candidates against COVID-19. *Journal of Biomolecular Structure and Dynamics*. https://doi.org/10.1080/07391102.2020.1762743

Wang, B., Guo, H., Ling, L., Ji, J., Niu, J., & Gu, Y. (2020). The chronic adverse effect of chloroquine on kidney in rats through an autophagy dependent and independent pathways. *Nephron, 144*(1), 53–64.

Wang, M., Cao, R., Zhang, L., Yang, X., Liu, J., Xu, M., & Xiao, G. (2020). Remdesivir and chloroquine effectively inhibit the recently emerged novel coronavirus (2019-nCoV) *in vitro. Cell Research, 30*(3), 269–271.

Wang, C., Horby, P. W., Hayden, F. G., & Gao, G. F. (2020). A novel coronavirus outbreak of global health concern. *The Lancet*, *395*(10223), 470–473.

Weiss, P., & Murdoch, D.R. (2020). Clinical course and mortality risk of severe COVID-19. *The Lancet, 395*(10229), 1014-1015.

Woo, P. C. Y., Lau, S. K. P., Chu, C-m., Chan, K-h., Tsoi, H-w., Huang, Y., Wong, B. H. L., Poon, R. W. S., Cai, J. J., Luk, W-k., Poon, L. L. M., Wong, S. S. Y., Guan, Y., Peiris, J. S. M., & Yuen, K-Y. (2005). Characterization and complete genome sequence of a novel coronavirus, coronavirus HKU1, from patients with pneumonia. *Journal of Virology*, *79*(2), 884–895.

World Health Organization. (2020). *Naming the coronavirus disease (covid-19) and the virus that causes it*.

Woźniak, Ł., Skąpska, S., & Marszałek, K. (2015). Ursolic acid- a pentacyclic triterpenoid with a wide spectrum of pharmacological activities. *Molecules, 20,* 20614-20641. doi: 10.3390/molecules201119721

Wu, F., Zhao, S., Yu, B., Chen, Y.M., Wang, W., Song, Z.G., Hu, Y., Tao, Z.W., Tian, J.H., Pei, Y.Y., Yuan, M.L., Zhang, Y.L., Dai, F.H., Liu, Y., Wang, Q.M., Zheng, J.J., Xu, L., Holmes, E.C., & Zhang, Y.Z. (2020). A new coronavirus associated with human respiratory disease in China. *Nature, 579* (7798), 265-269.

Xu, X., Chen, P., Wang, J., Feng, J., Zhou, H., Li, X., & Hao, P. (2020). Evolution of the novel coronavirus from the ongoing Wuhan outbreak and modeling of its spike protein for risk of human transmission. *Science China Life Sciences, 63*(3), 457–460.

Yang, H., Bartlam, M., & Rao, Z. (2006). Drug design targeting the main protease, the Achilles' Heel of coronaviruses. *Current Pharmaceutical Design*, *12*(35), 4573–4590. doi:10.2174/138161206779010369

Yu, W., & MacKerell AD, Jr. (2017). Computer-aided drug design methods. *Methods in Molecular Biology, 1520*, 85-106. doi: 10.1007/978-1-4939-6634-9_5.

Yuan, M., Yin, W., Tao, Z., Tan, W., & Hu, Y. (2020). Association of radiologic findings with mortality of patients infected with 2019 novel coronavirus in Wuhan, China. *PLoS One, 15*(3), e0230548.

Zhang, L., Lin, D., Sun, X., Curth, U., Drosten, U., Sauerhering, L., Becker, S., Rox, K., & Hilgenfeld, R. (2020). Crystal structure of SARS-CoV-2 main protease provides a basis for design of improved α-ketoamide inhibitors. *Science*, eabb3405.doi: 10.1126/science.abb3405.

Figures

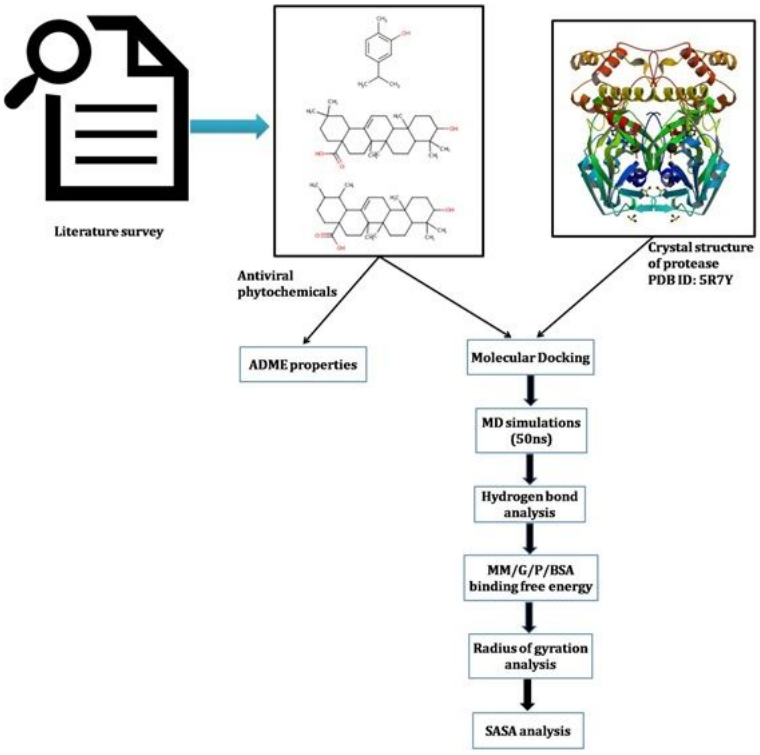

Figure 1

Flowchart of pipeline used in present study to identify the phytochemical based inhibitors of Mpro.

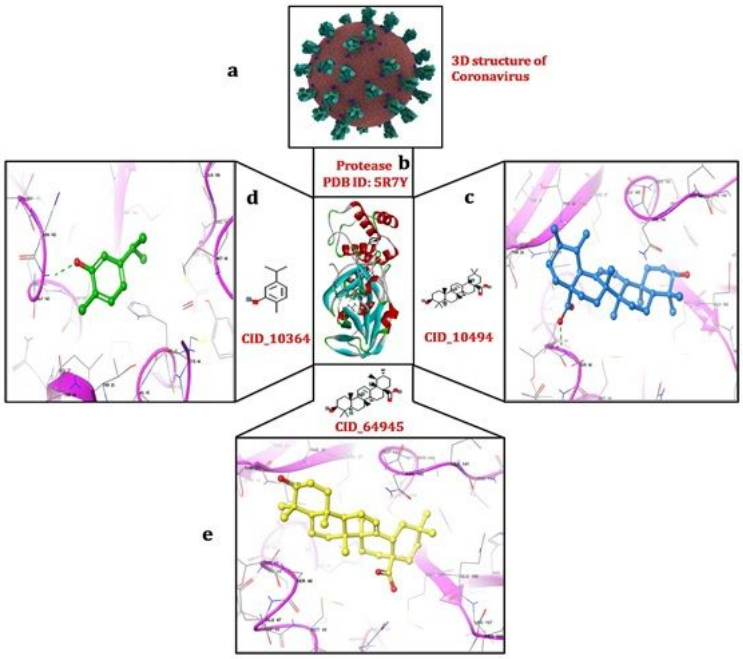

Figure 2

Schematic representation of molecular docking between Mpro and phytochemicals; (a) 3D structure of coronavirus derived from the RCSB-Protein Data Bank (PDB); (b) crystal structure of main protease of COVID-19 obtained from the PDB with PDB ID:5R7Y (c) interaction between Mpro and oleanolic acid with -6.0 kcal/mol docking energy; (d) interaction between Mpro and carvacrol with docking energy -4.0 kcal/mol; (e) interaction between Mpro and ursolic acid with -5.9 kcal/mol docking energy. Interactions were visualized using maestro and discovery studio programs.

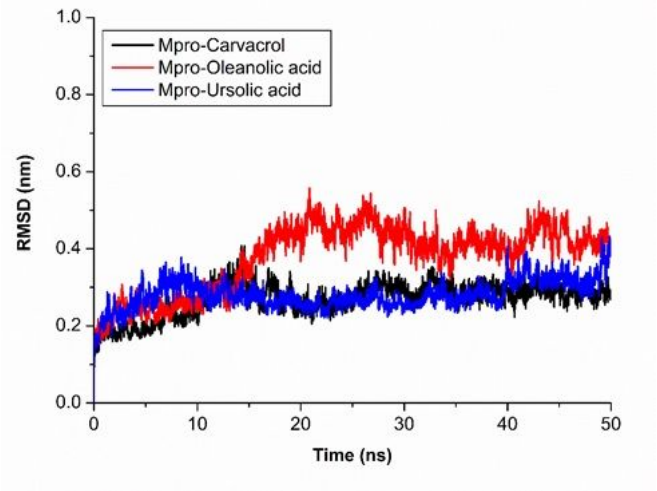

Figure 3

RMSD analysis of protein backbone during MD simulation.

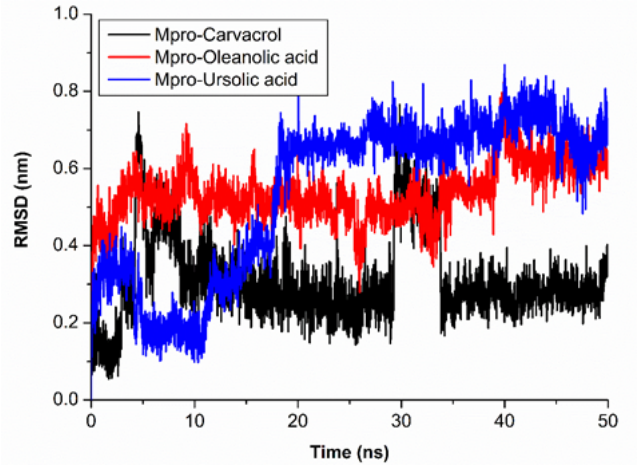

Figure 4

Analysis of RMSD of ligands and Mpro complexes; Mpro-carvacrol complex (Black), Mpro-oleanolic acid complex (Red), Mpro-ursolic acid complex (Blue).

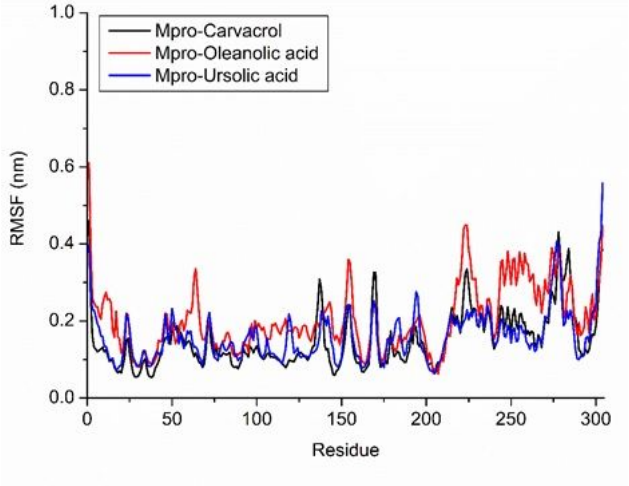

Figure 5

Analysis of RMSF of Cα during MD simulation; Mpro-carvacrol complex (Black), Mpro-oleanolic acid complex (Red), Mpro-ursolic acid complex (Blue).

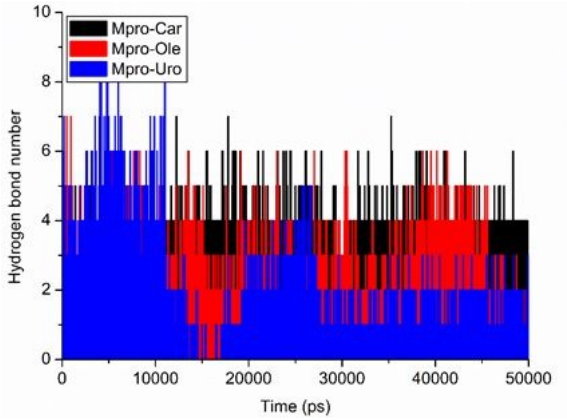

Figure 6

Intermolecular hydrogen bonds between the ligands and Mpro protein; Mpro-carvacrol complex (Black), Mpro-oleanolic acid complex (Red), Mpro-ursolic acid complex (Blue).

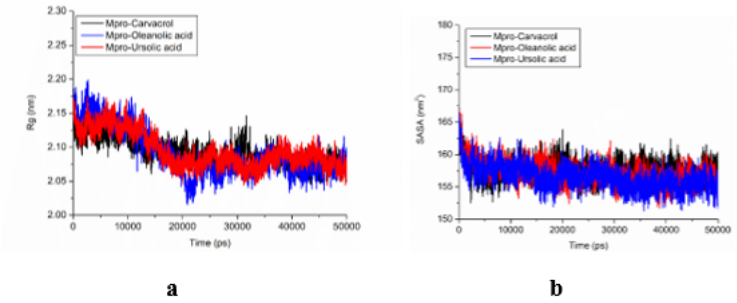

Figure 7

(a) Radius of gyration (Rg); Mpro-carvacrol complex (Black), Mpro-oleanolic acid complex (Blue), Mpro-ursolic acid complex (Red); (b) Solvent surface accessible area (SASA); Mpro-carvacrol complex (Black), Mpro-oleanolic acid complex (Red), Mpro-ursolic acid complex (Blue).